Phonons in the alloy superlattice GaAs-$Al_xGa_{1-x}As$

Akiko Kobayashi
Department of Physics and Astronomy, University of Maryland, College Park, Maryland 20742

A. Roy
Department of Physics, The City College of the City University of New York, New York, New York 10031
(Received 20 June 1986)

The densities of phonon states near wave vector $\mathbf{k}=\mathbf{0}$, projected onto basic vibrational states (i.e., x, y, or z vibrations of the cation or anion sublattice), are obtained for the alloy superlattice GaAs-$Al_xGa_{1-x}As$. Both confined and propagative optic phonons as well as folded acoustic phonons in the alloy superlattice are well accounted for. The results are compared with Raman data and the basic vibrations that give rise to principal features in the spectrum are identified.

I. INTRODUCTION

Recent developments in crystal-growth techniques (such as molecular-beam epitaxy or metalorganic chemical-vapor deposition) have stimulated studies of various aspects of semiconductor superlattices. This is largely due to the capability inherent in these techniques of controlling the spatial periodicity of the alternating semiconductor layers. Although, because of potential device applications of these superlattices, much attention has been paid to electronic properties, studies of vibrational properties are still at an early stage. However, Raman measurements on some GaAs-$Al_xGa_{1-x}As$ superlattices[1-6] have yielded novel spectral features. These features have been attributed to scattering from phonons near the center of a zone that has been folded because of the superlattice periodicity. In a bulk zinc-blende structure, with two atoms per unit cell, there are three acoustic modes (triply degenerate at $\mathbf{k}=\mathbf{0}$) and three optic modes (longitudinal-optic mode and doubly degenerate transverse-optic mode at $\mathbf{k}=\mathbf{0}$). On the other hand, a superlattice, with n_1 monolayers of one compound and n_2 monolayers of the other compound, has $2(n_1+n_2)$ atoms in a unit cell, and there are three acoustic modes and $6(n_1+n_2)-3$ optic modes. The symmetries and the irreducible representations of these modes depend on the character of each operation of the point group on the atoms of the unit cell, and thus depend on the number of monolayers per superlattice period. In the Raman studies on GaAs-$Al_xGa_{1-x}As$ superlattices,[1-6] the assignments of symmetry to the observed peaks were made by means of selection rules determined by the directions of the incident and scattered light polarizations. (For example, in a backscattering Raman measurement along the $z||[001]$ direction, with the incident and scattered light polarized along the $x||[100]$ direction, only the modes that have A_1 symmetry are selected, i.e., in-phase vibrations of the anion and cation sublattices along the z direction.) In this paper, instead, we look for the contribution of each basic vibration (the x, y, or z vibration of the cation or anion sublattice) to the density of phonon states of the superlattice (particularly at wave vector $\mathbf{k}=\mathbf{0}$). This type of calculation should provide information complementary to the results of Raman measurements in the study of phonons in superlattices.

We obtain the contribution of a basic vibration to the density of phonon states by calculating the projection of the density-of-states spectrum on to this vibrational state, for any specified wave vector $\mathbf{k}$. We do this employing the $\mathbf{k}$-space recursion method,[7-9] which is a slight modification of the orthodox real-space recursion method.[10] We specifically consider the case of the alloy superlattice GaAs-$Al_{0.3}Ga_{0.7}As$ with 15 monolayers of GaAs (~ 42 Å) and 3 monolayers of $Al_{0.3}Ga_{0.7}As$ (~ 8 Å) per period, and compare our results with the Raman data of Colvard *et al.*[6]

II. OUTLINE OF CALCULATION

The recursion method[10] is known to be well suited for obtaining densities of states of disordered systems. We have applied this method previously for obtaining densities of phonon states of semiconducting alloys, as described in Refs. 11–13, in which each of the principal features in the density-of-states spectra was associated with vibrations of specific local alloy clusters. The $\mathbf{k}$-space recursion method,[7-9] on the other hand, allows us to obtain the density of states at any specified wave vector, in particular, near $\mathbf{k}=\mathbf{0}$. It is thus expected to be useful in interpretation of data on elementary excitations in alloy superlattices obtained by use of long-wavelength probes.

We start with a Green's-function operator,

$$G(\omega)=\frac{1}{\omega^2-D}\ , \tag{1}$$

where D is the dynamical matrix in operator form. Using the complete basis set $|\mathbf{k},s\rangle$ (sth eigenstate with wave vector $\mathbf{k}$), Eq. (1) can be written as

$$G(\omega)=\sum_{\mathbf{k},s}\frac{|\mathbf{k},s\rangle\langle\mathbf{k},s|}{\omega^2-\omega_{\mathbf{k}s}^2}\ . \tag{2}$$

Each crystal eigenstate, $|\mathbf{k},s\rangle$, can be expressed as a linear combination of Bloch-type states, $|\mathbf{k},b,i\rangle$:

$$|\mathbf{k},s\rangle=\sum_{b,i}\langle\mathbf{k},b,i\,|\,\mathbf{k},s\rangle\,|\mathbf{k},b,i\rangle\ , \tag{3}$$

where

$$|\mathbf{k},b,i\rangle=N^{-1/2}\sum_{n}\exp(i\mathbf{k}\cdot\mathbf{R}_n)\,|n,b,i\rangle\ . \tag{4}$$

$|n,b,i\rangle$ is the local basis set which represents the i vibration ($i=x$, y, or z) of an atom of type b ($b=a$ for anion or c for cation) in the nth unit cell. In the real-space recursion method,[10] the quantity that can be obtained is the diagonal matrix element of $G(\omega)$ for a specific local state, $|n,b,i\rangle$, i.e., the local density of states in real space. In the **k**-space recursion method, however, we seek the diagonal matrix element of $G(\omega)$ for a specific Bloch-type state, $|\mathbf{k},b,i\rangle$:

$$d(\omega;\mathbf{k},b,i)=(-1/\pi)\mathrm{Im}\langle\mathbf{k},b,i\,|\,G(\omega)\,|\,\mathbf{k},b,i\rangle\ . \tag{5}$$

In employing the **k**-space recursion method, it should be kept in mind that one tacitly assumes that band structures (or phonon dispersion relations) are retained in alloys or alloy superlattices, although translational invariance no longer pertains and the Bloch theorem is invalid. It is also essential to impose periodic boundary conditions on the cluster generated in this method, so as to avoid spurious surface scattering. For the alloy superlattice GaAs-$Al_xGa_{1-x}As$, the cluster is made up of alternating layers of GaAs, with thickness d_1, and $Al_xGa_{1-x}As$, with thickness d_2, along the [001] crystal axis. The superlattice period is $d=d_1+d_2$. Denoting the size of the cluster in the z direction by L_z, the number of GaAs layers in a period by n_1, and the number of alloy layers in a period by n_2, we have

$$L_z=N_z d\ , \tag{6}$$

where N_z is the total number of periods in the z direction, and $d\sim(2.83\ \text{Å})\times(n_1+n_2)$. 2.83 Å is the monolayer spacing for GaAs-$Al_xGa_{1-x}As$ superlattices. Since the lattice constants for GaAs and AlAs are nearly equal, the lattice mismatch can be neglected, and a single (average) lattice constant assumed. The size of the Brillouin zone along the [001] direction is thus reduced to π/d, and the possible values of k_z in the reduced zone, as determined by the periodic boundary conditions of the cluster, are

$$k_z=(2\pi/d)(n/N_z)\quad(n=0,\pm1,\pm2,\ldots,\pm N_z/2)\ . \tag{7}$$

Here we consider the case of zone-center phonons in the alloy superlattice GaAs-$Al_{0.3}Ga_{0.7}As$, with the number of layers $(n_1,n_2)=(15,3)$ [thicknesses $(d_1,d_2)\cong(42\ \text{Å}, 8\ \text{Å})$].

We generate a cluster of 3600 atoms, containing a total of 18 monolayers in the z direction—15 monolayers of GaAs and 3 monolayers of $Al_{0.3}Ga_{0.7}As$. Each monolayer contains 10×10 anions and 10×10 cations in the x-y plane. This cluster corresponds to $N_z=1$ in Eqs. (6) and (7). Note that only a limited number of **k** vectors are consistent with the cluster size generated and the periodic boundary conditions imposed in the method [Eqs. (6) and (7)]. Ostensibly, by increasing the number of layers in the cluster, one can obtain the spectral densities of states at various values of k_z. However, the computer time required for larger clusters becomes a serious problem. The present choice of cluster size (15 layers of GaAs and 3 layers of $Al_xGa_{1-x}As$) corresponds to the case of having only one superlattice period in the cluster: only $k_z=0$, therefore, is allowed in the calculation.

The lattice dynamics of zinc-blende semiconductors have been considered previously,[11–13] employing the rigid-ion model with first-nearest-neighbor force constants, α and β, and second-nearest-neighbor force constants, λ_a, λ_c, μ_a, μ_c, ν_a, and ν_c, where a refers to the second-nearest-neighbor anion bond and c to the second-nearest-neighbor cation bond. Here we use the same notation and utilize, for the values of these parameters, those of bulk GaAs and AlAs that have been determined in Ref. 11. The distribution of Ga and Al atoms over the cation sites in the alloy layers is determined by use of a random number generator with $x=0.3$. The first-nearest-neighbor force constants, α and β, of pure GaAs and pure AlAs are used for Ga-As pairs and Al-As pairs in the cluster. The second-nearest-neighbor force constants for four possible pairs of atoms in the cluster are determined from

$$\begin{aligned}
&\lambda(\text{Ga-Ga})=\lambda_c(\text{GaAs})\ ,\\
&\lambda(\text{As-As})=[\lambda_a(\text{GaAs})+\lambda_a(\text{AlAs})]/2\ ,\\
&\lambda(\text{Al-Al})=\lambda_c(\text{AlAs})\ ,\\
&\lambda(\text{Ga-Al})=[\lambda_c(\text{GaAs})+\lambda_c(\text{AlAs})]/2\ .
\end{aligned} \tag{8}$$

We use the same relations for the other second-nearest-neighbor force constants, μ and ν, for the four possible pairs of atoms. We use the same averaged force constants for pairs of atoms in the entire structure, in keeping with the assumption of a single average lattice constant, without distinguishing between those in the GaAs layers and those in the alloy layers.

It should be mentioned here that a number of theoretical efforts have been made for the purpose of obtaining phonon dispersion relations in the GaAs-AlAs superlattice. For example, Yip and Chang[14] have extended the idea of complex band-structure calculations[15] to obtaining phonon dispersion relations for $(GaAs)_n$-$(AlAs)_m$ superlattices. In treating the lattice dynamics of the parent compounds, they used the bond-charge model and included long-range Coulomb forces by a perturbation method. Kanellis[16] has noted that an appropriate transformation and combination of dynamical matrices of the parent compounds results in a desired matrix for the superlattice, and has presented the dispersion relation for the $(GaAs)_4$-$(AlAs)_4$ superlattice. These approaches, however, are limited to pure GaAs-AlAs superlattices (without any alloy disorder), since they explicitly utilize the supercell-unit scheme and translational invariance for all the directions pertaining to the system in order to obtain the dynamical matrices. In contrast to the above approaches, our main purpose is to directly obtain contributions of specific vibrational states to the density of phonon states of the *alloy* superlattice GaAs-$Al_xGa_{1-x}As$. These spectral densities of states exhibit reasonable spectral weights and intensities

so that direct and meaningful comparison with Raman spectra can be made. The recursion method not only is well suited for density-of-states calculations for disordered systems, but also enables us to associate peaks in the density of phonon states with specific vibrational modes arising from specific local atomic arrangements, and to correlate those peaks with major features of Raman spectra. A possible drawback arises from the fact that the method requires a localized basis [such as the (x,y,z) basis of each atom in the rigid-ion model] on a finite cluster of atoms. Since the recursion method is a real-space cluster calculation, inclusion of the long-range Coulomb forces is computationally impractical. As a consequence, the longitudinal-optic (LO) and the transverse-optic (TO) modes are degenerate at $\mathbf{k}=0$ in the original first Brillouin zone (but not in the new folded zones). Due to the use of the rigid-ion model (which is known to be inferior to the shell model or the bond-charge model) as well as to the neglect of the long-range Coulomb forces, a quantitative listing of peak positions in the density of states is beyond the scope of the present calculation. We would like to emphasize, however, that by separately extracting the density of phonon states for in-plane vibrations and for vibrations normal to the layers, we can still obtain global spectral features associated with these modes. (This type of extraction is especially useful for optic modes, since it has been shown both theoretically[17] and experimentally[18] that, in the superlattice, in-plane vibrations are of TO character and vibrations normal to the layers are of LO character, regardless of the direction of the added wave vector.)

III. RESULTS AND DISCUSSION

Figures 1—4 show the densities of states calculated at $\mathbf{k}=0$, projected on to the states $|a,2^{-1/2}(x\pm y)\rangle$, $|a,z\rangle$, $|c,2^{-1/2}(x\pm y)\rangle$, and $|c,z\rangle$, respectively, where a and c specify the anion sublattice (As) and cation sublattice (Ga and Al). In the following, we discuss our results for the optic region and the acoustic region separately.

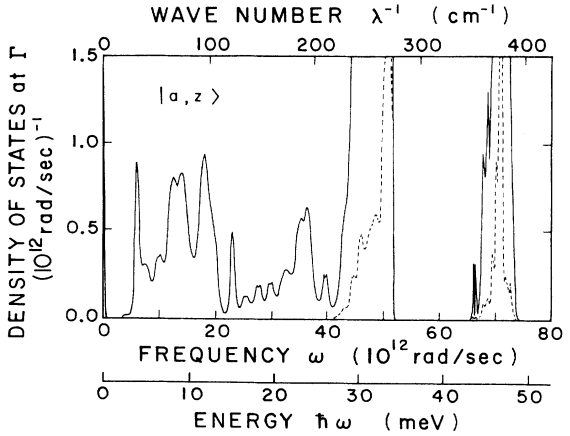

FIG. 2. Calculated density of states at the zone center, projected to the state $|a,z\rangle$. The optic bands, scaled down by a factor of 10, are indicated by the dashed lines.

A. Optic region (220—400 cm^{-1})

In Figs. 1—4, the two bands which show high intensities at ~ 270 cm^{-1} and at ~ 370 cm^{-1} originate from the GaAs-like optic vibrations and the AlAs-like optic vibrations, respectively. The dashed lines in the figures indicate these optic bands, scaled down by a factor of 10. In keeping with the fact that the mass of a Ga atom is nearly equal to that of an As atom, we see that the Ga vibrations in Figs. 3 and 4, and the As vibrations in Figs. 1 and 2 give rise to nearly the same spectral weights in the GaAs-like optic band (~ 270 cm^{-1}). On the other hand, it is seen that the cation vibrations in Figs. 3 and 4 give rise to higher spectral weights in the AlAs-like optic band (~ 370 cm^{-1}) than the As vibrations do (Figs. 1 and 2), because of the light Al atomic mass. The As vibrations, instead, contribute to the density-of-states spectra at the lower-frequency side ($0<\omega<220$ cm^{-1} in Figs. 1 and 2). The secondary peaks and shoulders seen in the two optic

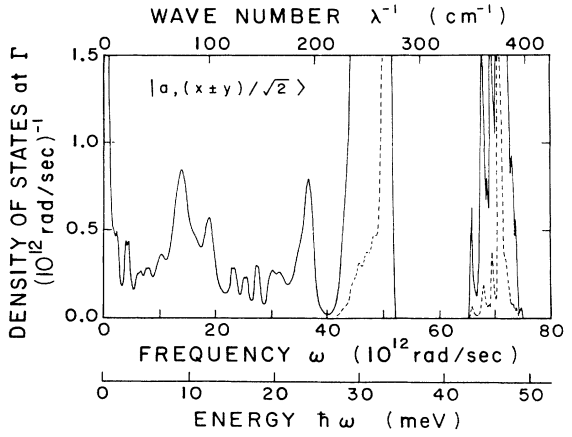

FIG. 1. Calculated density of states at the zone center, projected to the state $|a,2^{-1/2}(x\pm y)\rangle$. The optic bands, scaled down by a factor of 10, are indicated by the dashed lines.

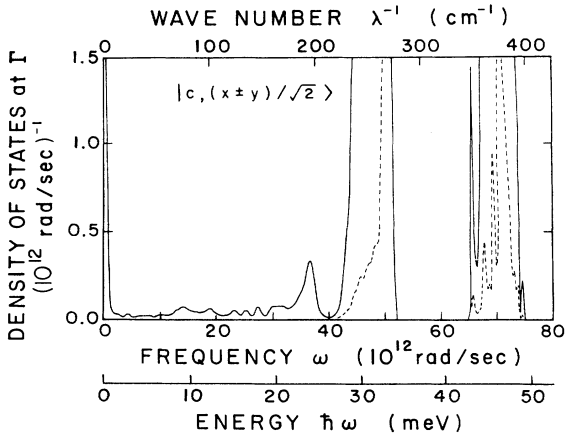

FIG. 3. Calculated density of states at the zone center, projected to the state $|c,2^{-1/2}(x\pm y)\rangle$. The optic bands, scaled down by a factor of 10, are indicated by the dashed lines.

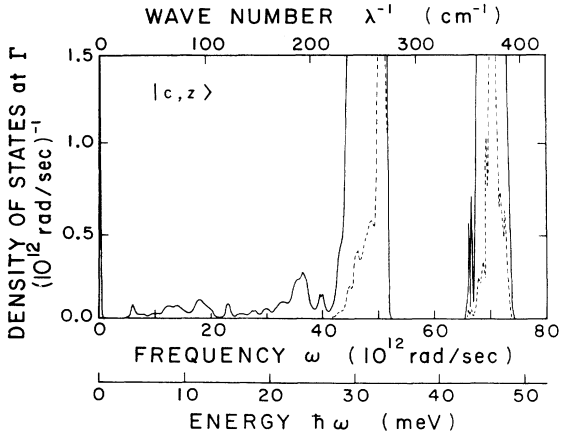

FIG. 4. Calculated density of states at the zone center, projected to the state $|c,z\rangle$. The optic bands, scaled down by a factor of 10, are indicated by the dashed lines.

bands are features that can be attributed to new modes arising from the superlattice structure and from alloy disorder.

It is now well accepted that the optic phonons of the GaAs-AlAs superlattice can be regarded as spatially localized in either the GaAs layer or the AlAs layer.[6,14,18,19] These phonons, in analogy with the quantization of electrons in potential wells, are termed confined optic phonons. Their frequencies are given by $\omega_m(\mathbf{k})=\omega(m\pi/d_i)$, where m is an integer and $d_{1(2)}$ is the thickness of the GaAs (AlAs) layer. Thus, these confined phonons produce flat dispersion branches due to their localization. In the alloy superlattice GaAs-$Al_xGa_{1-x}As$, however, both layers may support the GaAs-like optic vibrations, resulting in propagative waves with dispersive ω versus $\mathbf{k}$. Based on the projected densities of states in Figs. 1—4 and the densities of states obtained for the $Al_xGa_{1-x}As$ alloys in Ref. 11, we conclude that the GaAs-like optic band is comprised of "alloy modes" in addition to the pure GaAs optic vibrations. These alloy modes are the Ga vibrations with some Al atoms at the second-nearest-neighbor sites and the As vibrations with some Al atoms at the first-nearest-neighbor sites. These alloy modes contribute to the densities of states especially at the low-frequency side of the GaAs-like optic band. The overlap in energy between these alloy modes and the pure GaAs optic modes can thus produce propagative waves in both layers. Therefore, we conclude that the optic phonons giving rise to new features, that is the secondary peaks and shoulders at the low frequency side of the main GaAs-LO peak (Figs. 2 and 4) and of the main TO peak (Figs. 1 and 3), are not confined, but propagative.

On the other hand, the AlAs-like optic band exhibits distinct peaks separated in energy, as can be seen in Figs. 1—4. This is because of the thin $Al_xGa_{1-x}As$ layer (three monolayers) chosen in the calculation. Note that LO (or TO) phonons confined in the AlAs layer (or GaAs layer) in a GaAs-AlAs superlattice produce as many different modes as the number of monolayers in a unit cell.[14] Additional peaks in the AlAs-like optic region (in Figs. 1—4) as well as the shift and the broadening of the peaks arise from the alloy effect. Vibrations of Al atoms that have some second-nearest-neighbor Ga atoms are responsible for these features.[11] The Ga atoms affecting the Al vibrations may also be located in the GaAs layer but only near the interface. We conclude that the AlAs-like optic phonons in the alloy superlattice GaAs-$Al_xGa_{1-x}As$ are still confined in the $Al_xGa_{1-x}As$ layer in spite of the alloy disorder. The differences in the spectrum of the AlAs-like phonons of the alloy superlattice as compared to the pure GaAs-AlAs superlattice arise from the presence of Ga atoms in the alloy layer as well as just beyond the interface.

It should be noted here that Sood *et al.*[20] have observed new Raman structures in the optic region of GaAs-AlAs superlattices, in addition to those arising from the confined optic phonons. They assigned these new structures to interface vibrational modes. It was indicated[20] that these vibrations produce long-range electric fields in the GaAs layers, since the corresponding Raman structure resonates strongly with GaAs excitons. Unfortunately, the densities of states in Figs. 1—4 do not account for such interface vibrational modes. This is not because of our neglect of the long-range Coulomb forces, since the densities of states projected separately on to the z-vibrational state and to the $(x\pm y)$-vibrational state should manifest the anisotropic features of these interface vibrations. Taking into account the fact that these new Raman structures were observed only under strong resonant conditions, we make the conjecture that their mode strengths in the density of states is very weak, giving no distinct features in the calculated density-of-states spectra. Furthermore, the long-wavelength limit taken in the calculation poses difficulty in distinguishing between normal modes and interface vibrational modes. Additional data as well as a full microscopic lattice-dynamics calculation must be awaited for a further understanding of the nature of these modes.

B. Acoustic region (0—220 cm^{-1})

In the region from ~ 5 cm^{-1} to ~ 220 cm^{-1} in Figs. 1—4 we see new features which are not present in bulk GaAs or AlAs, but are again attributed to the superlattice structure and the alloy disorder. These phonon modes, although they are, in a strict sense, optic modes by nature, are commonly referred to as folded acoustic modes because they derive from bulk acoustic phonons. Only the modes giving rise to the peak at ~ 0 cm^{-1} are genuinely acoustic and originate from the zone-center acoustic modes of the bulk.

In Fig. 5 we display the Raman spectrum (top) obtained by Colvard *et al.*,[6] and the calculated densities of states (bottom) projected on to the state $|a,z\rangle$ (dashed) and to the state $|a,2^{-1/2}(x+y)\rangle$ (solid) in the low-frequency region at the zone center. The densities of states projected to the cation-sublattice space are not displayed here since the acoustic modes are comprised mainly of the vibrations of the heavy As atoms.

In comparing our results with the Raman data, we note that the densities of states which are calculated at $\mathbf{k}=\mathbf{0}$

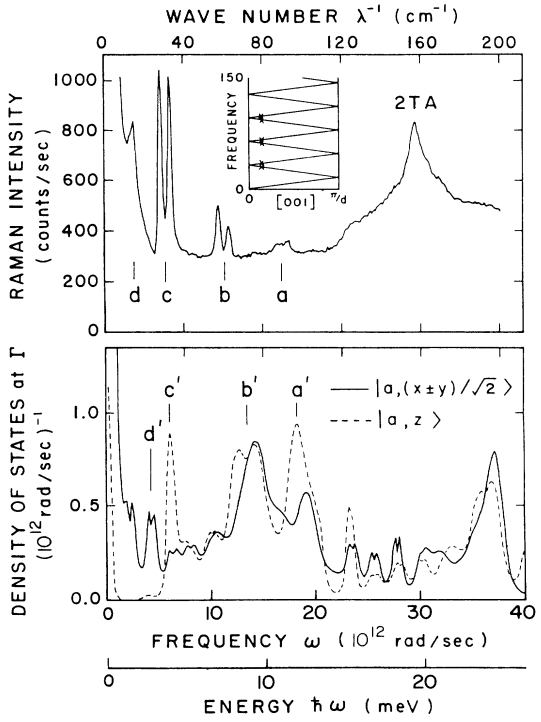

FIG. 5. Raman spectrum of LA phonons from Ref. 6 (top) for the GaAs-$Al_{0.3}Ga_{0.7}As$ superlattice with layer thicknesses (42 Å, 8 Å), along with the calculated densities of states (bottom) at the zone center for the same system, projected on to the states $|a,z\rangle$ (dashed line) and $|a,2^{-1/2}(x\pm y)\rangle$ (solid line). The inset shows the folded LA phonons obtained using the Rytov model (Ref. 21), as described in Ref. 6. The broad two-phonon contribution at ~ 160 cm^{-1} is designated as 2TA. The distinct doublets in the Raman spectrum are the effects of wave-vector transfer which needs to be taken as a finite quantity because of the reduced zone size of the superlattice.

actually represent the densities of states *near* $\mathbf{k}=\mathbf{0}$, because of the disorder which renders the labeling with wave vector $\mathbf{k}$ not strictly valid in the alloy superlattice. Such a situation can be illustrated as follows. If we take a path along $\mathbf{k}=(0,0,\zeta)$ with $\zeta\to 0$, the $x\pm y$ vibrations represent the transverse modes; and if we take a path along $\mathbf{k}=(\zeta,\zeta,\zeta)$ with $\zeta\to 0$, the $x\pm y$ vibrations represent a component of the longitudinal modes. Therefore, the spectral density of states projected on to $|a,2^{-1/2}(x\pm y)\rangle$ [Fig. 1 and Fig. 5 (bottom)], for example, contains a mixture of transverse modes from $\mathbf{k}=(0,0,\zeta)_{\zeta\to 0}$, longitudinal modes from $\mathbf{k}=(\zeta,\zeta,\zeta)_{\zeta\to 0}$, and some $x\pm y$ vibrations from other directions. This is why we see nonvanishing spectral weights in the region $120\ cm^{-1}<\omega<220\ cm^{-1}$ in the density of states for $|a,2^{-1/2}(x\pm y)\rangle$ [Fig. 1 and Fig. 5 (bottom)] and $|c,2^{-1/2}(x\pm y)\rangle$ (Fig. 3), even though none should exist at $\mathbf{k}=(0,0,\zeta)_{\zeta\to 0}$ if one simply folds the transverse-acoustic (TA) branches of bulk GaAs or AlAs along the Γ–X zone.

We also note that the boson thermal factor, $n(\omega,T)+1$ (T is the temperature), provides increasingly higher weights as ω tends to 0 in the usual Raman spectrum. This effect is especially important here since interesting zone-folding effects take place in the acoustic region. However, it has been found[6] that, after correcting for this factor, the intensity of the first folded peak is only 0.01–0.13 times the GaAs-like longitudinal optic (LO) peak intensity, in agreement with the large difference in intensity (about a factor of 20 in Figs. 1–4) between the optic peaks and the acoustic peaks in our calculated spectral densities of states.

In Fig. 5 we immediately notice that the three main peaks in the density-of-states spectrum projected to the state $|a,z\rangle$, denoted by a', b', and c', correspond to the three folded phonon peaks in the data, marked by a, b, and c. As mentioned earlier, the $|a,z\rangle$-state spectrum includes vibrational modes not only from the [001] direction but also from other directions. The observed longitudinal-acoustic (LA) phonons, therefore, constitute a subset of the calculated $|a,z\rangle$-state spectrum. The splitting in the a, b, and c peaks, evident in the data, does not appear in the a', b', and c' peaks. This is because of the overlap of vibrational modes from various directions. In spite of the broadening due to the alloy disorder, the projected density of states on to the state $|a,z\rangle$ well accounts for the observed spectrum. Since the vibrations of As atoms provide the major contribution to the spectrum, it is confirmed that the acoustic modes are indeed propagative in both the GaAs and $Al_xGa_{1-x}As$ layers so that the usual description using the concept of zone folding (not confined modes) is appropriate in this frequency region.

In the frequency range from ~ 120 cm^{-1} to ~ 160 cm^{-1} in the calculated spectra, we see some peaks which show a small splitting. Each of these peaks arises from phonons from a particular direction (without overlap with modes from various other directions), and very close to $\mathbf{k}=\mathbf{0}$. This splitting should increase as one moves away from $\mathbf{k}=\mathbf{0}$, as is observed in the Raman spectrum. It should be mentioned here that this small splitting seen in some of the peaks in the calculated spectra is an intrinsic feature caused by the Bragg reflection of phonons at the zone center (and zone edges).

The lowest-energy peak, d, in the data, which does not correspond to a folded LA phonon,[6] is interesting. There seem to be two possible mechanisms that could give rise to this peak: one is plasmons and the other is vibrations in the plane of layers. Although the sample was not intentionally doped, the collective motion of residual electrons in the GaAs layers could give rise to a plasmon peak at a frequency of the order of several meV. On the other hand, our calculated density-of-states spectrum exhibits two low-energy peaks that arise from $|x\pm y\rangle$ vibrations: the peak indicated by d' and the peak at ~ 13 cm^{-1}. Although the peak position does not agree very well with that of the observed peak d, our results indicate that an in-plane vibration of As atoms could be Raman activated because of the breakdown of the selection rules, due either to the slight deviation from strict backscattering geometry or to the disorder-induced scattering which allows phonons with $\mathbf{k}$ vectors in any direction. In view of the fact that, unlike phonon frequencies, plasmon frequencies depend strongly on magnetic field (magnetoplasmons[22,23]),

measurements in the presence of an applied magnetic field would be of assistance in distinguishing between the two possibilities.

IV. CONCLUSIONS

The densities of states near wave vector $\mathbf{k}=0$, projected on to specific vibrational states, are obtained for the GaAs-$Al_xGa_{1-x}As$ superlattice. Since the lattice dynamics to describe phonons in the parent semiconductor compounds was limited to short-range forces,[11-13] accurate predictions for mode frequencies and precise descriptions of the LO-TO splitting at $\mathbf{k}=0$ are beyond the scope of the present calculations. However, by obtaining the density of states projected to each of the basic vibrational states, one can acquire some information as to which type of vibrations participate in giving rise to any specific peak in the density-of-states spectra. Based on the projected densities of states in the present work and the densities of states for $Al_xGa_{1-x}As$ alloys obtained in Ref. 11, we show that the secondary peaks and shoulders that appear in the low-frequency region of the GaAs-like optic band originate from alloy modes (vibrations of Ga and As with some Al atoms at the neighboring sites) in addition to pure GaAs optic modes. Therefore, GaAs-like optic modes in this region are propagative, not confined in the GaAs layer. On the other hand, we show that the AlAs-like optic modes are comprised mostly of Al-vibrations which, although perturbed by neighboring Ga atoms, result in confined phonons in the $Al_xGa_{1-x}As$ layer. As for the acoustic modes, our calculated density of states projected on to the As-sublattice space accounts well for the observed folded LA phonons.[6] Since some nominally Raman-inactive modes could appear in Raman spectra due either to disorder activation or to deviations from strict backscattering, individual components of the density of states help in the interpretation of such unexpected peaks in data. In this regard, our results indicate that the lowest-energy peak in the Raman data[6] of Fig. 5, which does not correspond to a folded LA phonon, could arise from vibrations in the plane of the superlattice layers. This peak could also be due to plasmons: measurements in a magnetic field may help resolve this issue.

ACKNOWLEDGMENTS

This work was supported by the Department of Energy [during the stay of one of us (A.K.) in the University of Illinois] and the U.S. Office of Naval Research. The work at City College was supported by the Department of Energy under Grant No. DE-FG02-84ER45153.

[1]A. S. Barker, Jr., J. L. Merz, and A. C. Gossard, Phys. Rev. B **17**, 3181 (1978).
[2]R. Merlin, C. Colvard, M. V. Klein, H. Morkoç, A. Y. Cho, and A. C. Gossard, Appl. Phys. Lett. **36**, 43 (1980).
[3]C. Colvard, R. Merlin, M. V. Klein, and A. C. Gossard, Phys. Rev. Lett. **45**, 298 (1980).
[4]J. Sapriel, J. C. Michel, J. C. Toledano, R. Vacher, J. Kervarec, and A. Regreny, Phys. Rev. B **28**, 2007 (1983).
[5]M. V. Kelin, C. Colvard, R. Fischer, and H. Morkoç, J. Phys. (Paris) Colloq. **C5**-131 (1984).
[6]C. Colvard, T. A. Grant, M. V. Klein, R. Merlin, R. Fischer, H. Morkoç, and A. C. Gossard, Phys. Rev. B **31**, 2080 (1985); C. Colvard, Ph.D. thesis, University of Illinois at Urbana-Champaign, 1984 (unpublished).
[7]T. Fujiwara and Y. Tanabe, J. Phys. F **9**, 1085 (1979).
[8]Y. Ishii and T. Fujiwara, J. Phys. F **10**, 2125 (1980).
[9]L. C. Davis, Phys. Rev. B **28**, 6961 (1983).
[10]R. Haydock, in *Solid State Physics*, edited by H. Ehrenreich, F. Seitz, and D. Turnbull (Academic, New York, 1980), Vol. 35, p. 215; M. J. Kelly, *ibid.*, Vol. 35, p. 296; V. Heine, *ibid.*, Vol. 35, p. 1; C. M. M. Nex, J. Phys. A **11**, 653 (1978); Comput. Phys. Commun. **34**, 101 (1984).
[11]A. Kobayashi, J. D. Dow, and E. P. O'Reilly, Superlatt. Microstruct. **1**, 471 (1985).
[12]A. Kobayashi, K. E. Newman, and J. D. Dow, Phys. Rev. B **32**, 5312 (1985).
[13]A. Kobayashi and A. Roy, Phys. Rev. B (to be published); A. Kobayashi, Ph.D. thesis, University of Illinois at Urbana-Champaign, 1985 (unpublished).
[14]S. Yip and Y. C. Chang, Phys. Rev. B **30**, 7637 (1984).
[15]J. N. Shulman and Y. C. Chang, Phys. Rev. B **24**, 4445 (1981); Y. C. Chang, *ibid.* **25**, 605 (1982); Y. C. Chang and J. N. Shulman, *ibid.* **25**, 3975 (1982).
[16]G. Kanellis, Solid State Commun. **58**, 93 (1986).
[17]G. Kanellis, J. F. Morhange, and M. Balkanski, Phys. Rev. B **28**, 3406 (1983).
[18]J. E. Zucker, A. Pinczuk, D. S. Chemla, A. Gossard, and W. Wiegmann, Phys. Rev. Lett. **53**, 1280 (1984).
[19]A. K. Sood, J. Menéndez, M. Cardona, and K. Ploog, Phys. Rev. Lett. **54**, 2111 (1985).
[20]A. K. Sood, J. Menéndez, M. Cardona, and K. Ploog, Phys. Rev. Lett. **54**, 2115 (1985).
[21]S. M. Rytov, Akust. Zh. **2**, 71 (1956) [Sov. Phys.—Acoust. **2**, 68 (1956)].
[22]S. Das Sarma, Phys. Rev. B **28**, 2240 (1983), and references therein.
[23]J. K. Jain, Phys. Rev. B **32**, 5456 (1985); and (private communications).